EsiB, a Novel Pathogenic *Escherichia coli* Secretory Immunoglobulin A-Binding Protein Impairing Neutrophil Activation

Ilaria Pastorello,[a] Silvia Rossi Paccani,[a] Roberto Rosini,[a] Rossella Mattera,[a] Mario Ferrer Navarro,[b] Dunja Urosev,[b] Barbara Nesta,[a] Paola Lo Surdo,[a] Mariangela Del Vecchio,[a] Valentina Rippa,[a] Isabella Bertoldi,[a] Danilo Gomes Moriel,[c] Alexander J. Laarman,[d] Jos A. G. van Strijp,[d] Xavier Daura,[b,e] Mariagrazia Pizza,[a] Laura Serino,[a] Marco Soriani[a]

Novartis Vaccines and Diagnostics Srl, Siena, Italy[a]; Institute of Biotechnology and Biomedicine (IBB), Universitat Autònoma de Barcelona (UAB), Bellaterra, Spain[b]; School of Chemistry and Molecular Biosciences, University of Queensland, Brisbane, Australia[c]; Department of Medical Microbiology, University Medical Center (UMC) Utrecht, Utrecht, The Netherlands[d]; Catalan Institution for Research and Advanced Studies (ICREA), Barcelona, Spain[e]

ABSTRACT **In this study, we have characterized the functional properties of a novel *Escherichia coli* antigen named EsiB (*E. coli* secretory immunoglobulin A-binding protein), recently reported to protect mice from sepsis. Gene distribution analysis of a panel of 267 strains representative of different *E. coli* pathotypes revealed that *esiB* is preferentially associated with extraintestinal strains, while the gene is rarely found in either intestinal or nonpathogenic strains. These findings were supported by the presence of anti-EsiB antibodies in the sera of patients affected by urinary tract infections (UTIs). By solving its crystal structure, we observed that EsiB adopts a superhelical fold composed of Sel1-like repeats (SLRs), a feature often associated with bacterial proteins possessing immunomodulatory functions. Indeed, we found that EsiB interacts with secretory immunoglobulin A (SIgA) through a specific motif identified by an immunocapturing approach. Functional assays showed that EsiB binding to SIgA is likely to interfere with productive FcαRI signaling, by inhibiting both SIgA-induced neutrophil chemotaxis and respiratory burst. Indeed, EsiB hampers SIgA-mediated signaling events by reducing the phosphorylation status of key signal-transducer cytosolic proteins, including mitogen-activated kinases. We propose that the interference with such immune events could contribute to the capacity of the bacterium to avoid clearance by neutrophils, as well as reducing the recruitment of immune cells to the infection site.**

IMPORTANCE **Pathogenic *Escherichia coli* infections have recently been exacerbated by increasing antibiotic resistance and the number of recurrent contagions. Attempts to develop preventive strategies against *E. coli* have not been successful, mainly due to the large antigenic and genetic variability of virulence factors, but also due to the complexity of the mechanisms used by the pathogen to evade the immune system. In this work, we elucidated the function of a recently discovered protective antigen, named EsiB, and described its capacity to interact with secretory immunoglobulin A (SIgA) and impair effector functions. This work unravels a novel strategy used by *E. coli* to subvert the host immune response and avoid neutrophil-dependent clearance.**

Received 24 April 2013 **Accepted** 24 June 2013 **Published** 23 July 2013

Citation Pastorello I, Rossi Paccani S, Rosini R, Mattera R, Ferrer Navarro M, Urosev D, Nesta B, Lo Surdo P, Del Vecchio M, Rippa V, Bertoldi I, Gomes Moriel D, Laarman AJ, van Strijp JAG, Daura X, Pizza M, Serino L, Soriani M. 2013. EsiB, a novel pathogenic *Escherichia coli* secretory immunoglobulin A-binding protein impairing neutrophil activation. mBio 4(4):e00206-13. doi:10.1128/mBio.00206-13.

Editor Philippe Sansonetti, Institut Pasteur

Address correspondence to Marco Soriani, marco.soriani@novartis.com.

Escherichia coli is able to colonize the human gastrointestinal tract soon after birth, often persisting for decades and providing mutual benefit to the host and bacterium. Although *E. coli* strains are usually regarded as commensals, certain isolates have acquired specific virulence traits that confer the ability to colonize new niches and to cause a wide variety of diseases (1). Pathogenic *E. coli* strains can be classified as either intestinal (InPEC) or extraintestinal (ExPEC), depending on the site of infection (2). The ability of *E. coli* to cause a wide range of diseases is partly due to its variable genome and its ability to gain or lose virulence attributes by horizontal gene transfer.

Host defense against pathogenic *E. coli* colonization of mucosal surfaces depends at least in part on the role of secretory immunoglobulin A (SIgA) and other opsonins in preventing bacterial adherence. SIgA is a hydrophilic, negatively charged molecule due to the predominance of hydrophilic amino acids in its Fc region and to the abundant glycosylation of both IgA and its secretory component. Therefore, SIgA can surround microorganisms with a hydrophilic shell that is repelled by the mucin glycocalyx at mucosal surfaces. SIgA is also able to agglutinate microbes and interfere with bacterial motility by interacting with flagella. In addition, SIgA interacts with bacterial products such as enzymes and toxins, neutralizing their action (3). Although IgA has so far been considered an anti-inflammatory antibody, recent data support its capacity to trigger a plethora of inflammatory functions by interacting with the myeloid IgA Fc receptor FcαRI (CD89), which is constitutively expressed on cells of the myeloid lineage, including neutrophils, monocytes, and macrophages (4). Al-

TABLE 1 Distribution of *esiB* gene among pathogenic and nonpathogenic strains

Pathotype	No. positive	Total no.	Prevalence, %
ExPEC	29	119	24.3
InPEC	6	117	5.1
Nonpathogenic	1	31	3.2
All	36	267	13.4

though mucosal immunity is crucial to the control of *E. coli* infections, no IgA-binding proteins (IgA-BPs) have been so far reported for any of the pathotypes.

Recently, a comparative genome analysis of ExPEC and nonpathogenic *E. coli* strains, named subtractive reverse vaccinology, led to the identification of nine potential vaccine candidates able to confer protection in a murine model of sepsis (5). Although some of the protective antigens have already been functionally described in the literature (6, 7), most of them have been assigned only putative or hypothetical functions; therefore, their experimental characterization could contribute to a greater understanding of ExPEC pathogenesis.

In this study, we present data on the functional characterization of the protective antigen c5321 (5) as a novel *E. coli* Sel1-like repeat (SRL) protein able to bind SIgA and inhibit its effector functions. This antigen has been named EsiB (*E. coli* secretory immunoglobulin A-binding protein), and it potentially contributes to ExPEC evasion of the host immune system.

RESULTS

The *esiB* gene is preferentially associated with ExPEC isolates. The presence of the *c5321* gene, here named *esiB*, was evaluated by PCR and bioinformatics analyses in a collection of 267 strains representative of different *E. coli* pathotypes, including 119 ExPEC, 117 InPEC, and 31 nonpathogenic strains. This panel comprised both isolates and complete genome sequences available in the NCBI database of human ($n = 190$) and animal ($n = 77$) origin (see Table S1 in the supplemental material). This analysis revealed that the gene was preferentially associated with ExPEC strains (29/119, 24.3%), while it was found in only a very low number of InPEC (6/117, 5.1%) and nonpathogenic (1/31, 3.2%) strains (Table 1). Moreover, multilocus sequence typing (MLST) and ancestral group analysis of the strains PCR positive for EsiB revealed that the gene was almost exclusively related to B2 strains, while its presence was not associated with a specific sequence type (see Fig. S1 and Table S1).

Genome sequence analysis of the *esiB* locus indicated that the gene was flanked by genes of unknown or putative functions (Fig. 1A). When absent, the ChpBS toxin-antitoxin system was

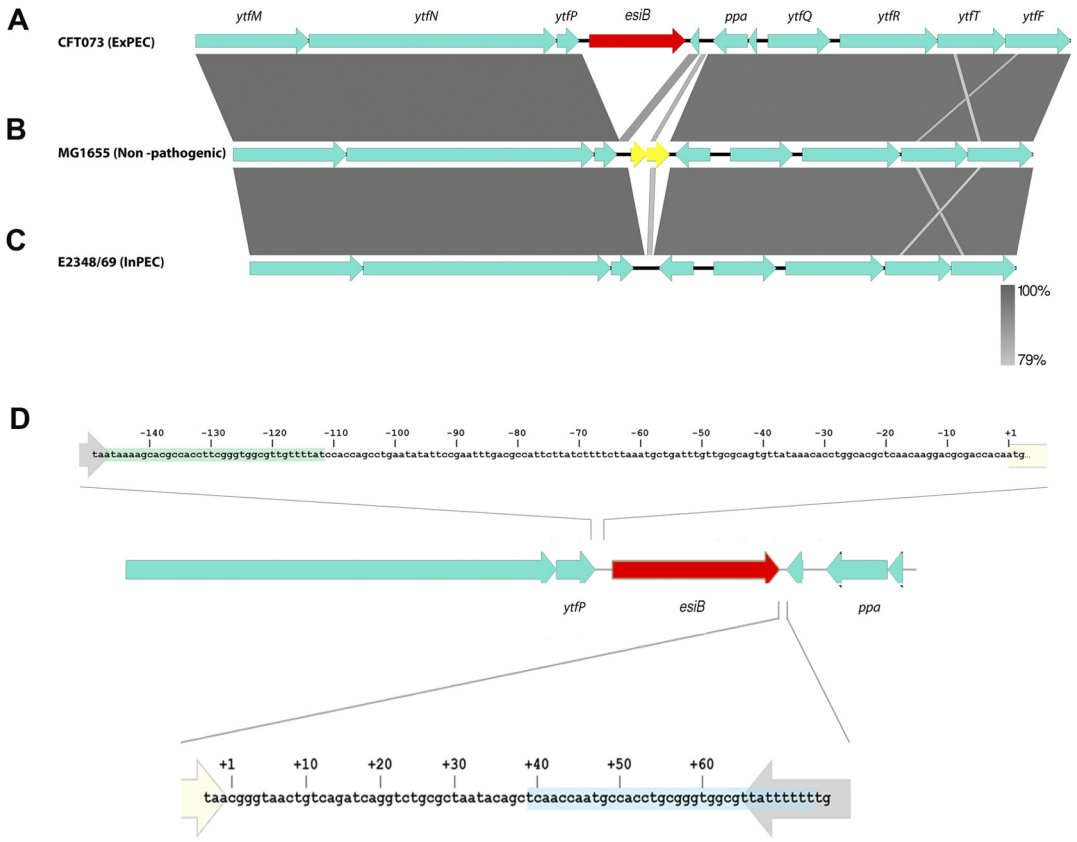

FIG 1 Genome sequence analysis of *esiB* locus. (A to C) In extraintestinal pathogenic *E. coli* (ExPEC) strain CFT073, the *esiB* gene (red arrow) is flanked by genome regions composed of conserved genes (blue arrows). The *esiB* upstream genes (*ytfM*, *ytfN*, and *ytfP*) are annotated as hypothetical proteins, while genes downstream of *esiB* (*ppa* and *ytfQ* to *ytfF*) are coding for the membrane component of a putative sugar ABC transporter system (A). When *esiB* is absent, in the K-12 nonpathogenic strain MG1655, the ChpBS toxin-antitoxin system (yellow arrows) can be found in the same context (B), but in several intestinal pathogenic (InPEC) strains, both *esiB* and *chpBS* genes are absent (C). (D) Graphical representation of the *esiB* gene region flanked by short direct repeats.

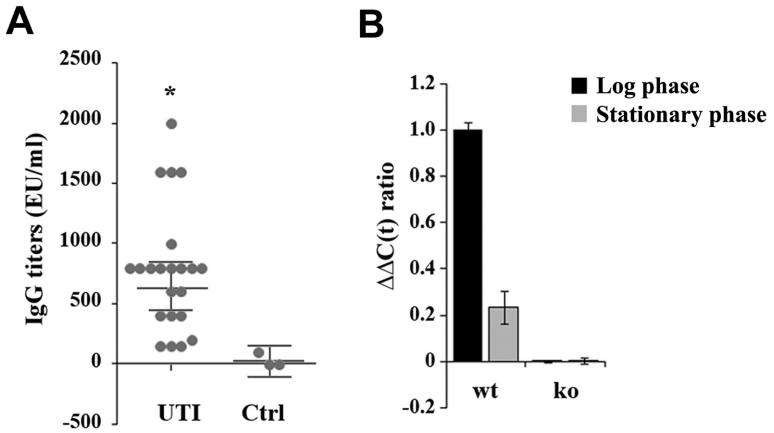

FIG 2 EsiB is recognized by human sera. (A) Immunoreactivity of human sera from UTI patients toward recombinant EsiB. ELISA was performed by applying the recombinant antigen as a coating on microtiter plates and overlaying wells with specific human sera. IgG binding was revealed by alkaline phosphatase-conjugated goat anti-human IgG. Sera from healthy human volunteers were used as IgG control levels. The data represent the means ± standard deviations of 22 human sera. Titers are reported as serum dilutions. *, comparison of EsiB IgG titers between healthy human volunteers and UTI patients: $P \leq 0.05$ (paired Student's *t* test). (B) EsiB expression under *in vitro* conditions. EsiB expression in UPEC strain CFT073 (wild type [wt]) grown in LB medium was evaluated by real-time quantitative PCR, using the isogenic mutant strain CFT073Δ*esiB* (ko) as a negative control. For relative quantification of gene expression, the starting mRNA copy number of the unknown samples was determined using the comparative $\Delta\Delta C_T$ method, and levels of the different transcripts were normalized to 16S rRNA, used as a housekeeping gene. The graph, representing a typical experiment out of two performed with similar results, shows that EsiB expression is higher in logarithmic phase than in stationary phase.

found in the same locus (Fig. 1B), but in several strains, both *esiB* and *chpBS* genes were absent (Fig. 1C). Of interest, the *esiB* gene was edged by short direct repeats with a partial inverted symmetry (Fig. 1D), suggesting that a homologous recombination event might have occurred. In the complete genomes analyzed where *esiB* was absent, only one copy of the repeat was found. The analysis of 47 complete *E. coli* genomes present in the NCBI databases revealed that 32% of strains lacked both *esiB* and *chpBS* genes, while 53% contained the *chpBS* gene and 15% contained the *esiB* gene.

EsiB is expressed *in vivo* during UTIs. To evaluate the immunogenicity of EsiB *in vivo* and to confirm its expression during key events of *E. coli* pathogenesis, we collected a panel of 22 sera from patients suffering from urinary tract infections (UTIs) and measured IgG titers against the antigen by enzyme-linked immunosorbent assay (ELISA). As shown in Fig. 2A, serum IgG titers in UTI patients were significantly higher than those of healthy human donors, suggesting that EsiB is immunogenic and expressed *in vivo* during *E. coli* infections. Moreover, immunoblot analysis revealed that recombinant EsiB was specifically recognized by a mouse antiserum raised by immunizing animals subcutaneously with live bacteria, indicating that the antigen is immunogenic during *in vivo* challenge (see Fig. S2 in the supplemental material). To define the kinetics of EsiB expression under *in vitro* conditions, we evaluated the mRNA levels in the uropathogenic strain CFT073 grown in Luria-Bertani (LB) medium by real-time quantitative PCR, and we observed that antigen expression was higher in logarithmic phase than in stationary phase (Fig. 2B). A time course analysis of bacteria grown in minimal medium revealed that the level of EsiB transcript remained constant up to 3 h of incubation (exponential phase) and declined during stationary phase (from 4 to 7 h) (see Fig. S3). Although *esiB* transcription was confirmed *in vitro*, the protein was not detected under any culture condition tested (data not shown), suggesting that *in vitro* mRNA levels in CFT073 might be insufficient to produce a detectable amount of the protein. However, confocal immunofluorescence microscopy of paraffin-embedded bladder sections derived from mice transurethrally infected with CFT073 revealed that EsiB is specifically expressed by bacteria associated with the bladder tissue (Fig. 3B). No signal was detected by using a serum raised by immunizing mice with adjuvant alone (Fig. 3A). Of interest, the staining was not evident in all bacteria and anti-EsiB antibodies appeared to recognize the protein at bacterial poles, suggesting a specific localization (Fig. 3C). Imaging data are representative of a qualitative imaging analysis of 10 bladder sections. In addition, by engineering an *E. coli* BL21(DE3) strain for the overexpression of EsiB under the control of an inducible promoter, we confirmed by both flow cytometry and confocal microscopy analysis (Fig. 4) that the antigen was exposed on the bacterial surface, suggesting that specific expression regulatory events may occur during *in vivo* infection. Moreover, when we performed Western blotting of the secreted faction from the BL21::*esiB* strain, we observed no presence of the protein (data not shown), suggesting that EsiB exerts its activity on the bacterial surface, although it cannot be excluded that, during *in vivo* infection, the protein may be released by bacteria undergoing stress conditions.

EsiB binds to human SIgA by a specific motif. By solving the crystal structure of EsiB (Protein Data Bank [PDB] entry 4BWR) (D. Urosev, M. Ferrer-Navarro, I. Pastorello, E. Cartocci, L. Costenaro, D. Zhulenkovs, J. D. Maréchal, A. Leonchiks, D. Reverter, L. Serino, M. Soriani, X. Daura, submitted for publication), we observed that the antigen is composed of 11 SLRs (residues 16 to 408), an N-terminal and two C-terminal capping helices, and a (partly helical) C-terminal tail. Considering that SLR proteins have been reported to be involved in immunomodulatory functions and immune evasion strategies (8) and that SIgA has been shown to play a major role in the host response to UTIs (9), we tested the capacity of recombinant EsiB to interact with human SIgA. ELISAs showed that EsiB binds to SIgA through a dose-dependent mechanism, with an estimated dissociation con-

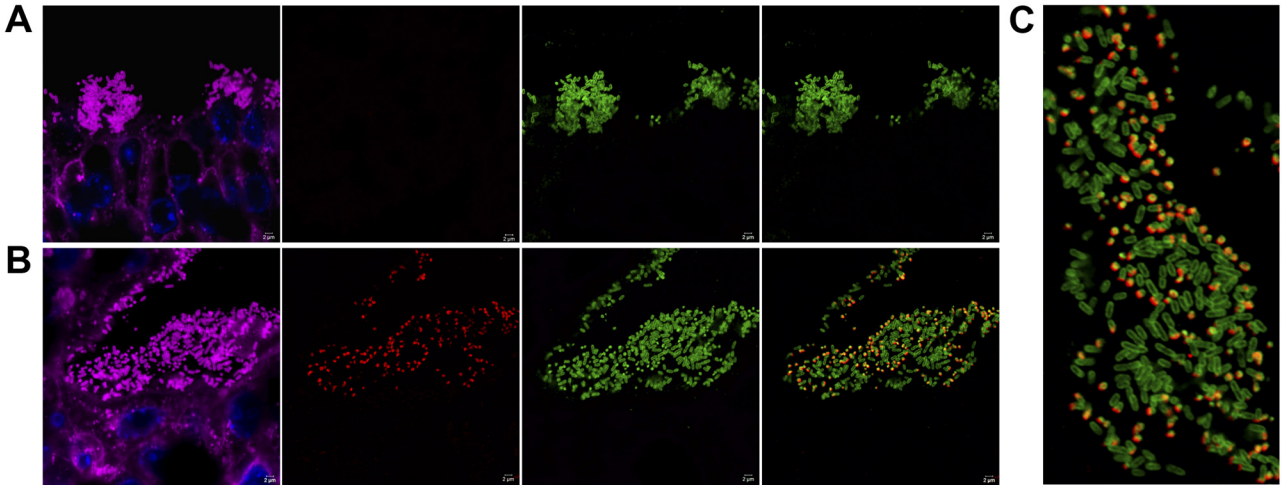

FIG 3 EsiB is expressed on the *E. coli* surface *in vivo*. Confocal imaging analysis of EsiB expression in bladder from mice infected with the CFT073 strain. Tissue sections embedded in paraffin were stained with WGA conjugated with Alexa Fluor 647 (violet), while the CFT073 strain was detected using a polyclonal serum raised against inactivated whole bacteria (green). An antiserum raised against the adjuvant alone was used as a negative control (A), while EsiB was stained with a specific rabbit antiserum (B) (red signal). The images are representative of multiple observations, from at least 10 sections. (C) Magnification of EsiB expression in bacteria colonizing the bladder. Staining of bacteria was performed as described for panel A.

stant (K_d) of approximately 10^{-7} M (Fig. 5A). Binding of EsiB to SIgA was confirmed by surface plasmon resonance (SPR) experiments. In brief, SIgA antibodies were covalently immobilized on a CM5 sensor chip via amine coupling and the interaction of increasing concentrations of the recombinant EsiB protein was monitored. The affinity between EsiB and SIgA was calculated by fitting the resulting curves with a 1:1 binding model, revealing an estimated dissociation constant (K_d) of 3×10^{-7} M (Fig. 5B).

To map the IgA-binding site on EsiB, we used an immunocapturing approach that employed superparamagnetic beads (Dynabeads). SIgA was coupled to the surface of the beads, which were then used to capture the EsiB peptide derived from partial digestion of the antigen with trypsin or with GluC in ammonium bicarbonate buffer. Following tryptic digestion, SIgA captured a single peptide with an *m/z* of 1,881.968 (Fig. 6), which by tandem mass spectrometry (MS/MS) analysis (data not shown) was identified as the fragment 244-VLFSQSAEQGNSIAQFR-260. Digestion with GluC in ammonium bicarbonate buffer resulted in no peptides being captured. In bicarbonate buffer, GluC cuts only after E residues. Therefore, this result suggests that residue E251 and its immediate neighbors might play an important role in the interaction between SIgA and EsiB. Importantly, the peptide relative to the SIgA-binding site is conserved among sequenced pathogenic *E. coli* strains.

EsiB inhibits the SIgA effector functions mediated by neutrophil receptor FcαRI. SIgA, which is the predominant antibody present in the secretions from mucosal surfaces of the genitourinary tract (10), has been shown to play a major role, together with polymorphonuclear neutrophils (PMNs), in the host response to UTIs (9). Indeed, SIgA can initiate numerous immune effector functions via the neutrophil IgA receptor FcαRI, leading to a plethora of potent eradication mechanisms, such as the production of reactive oxygen species (ROS) and the release of cytokines, chemotactic factors, and inflammatory lipid mediators (11). Therefore, in order to study the biological significance of EsiB

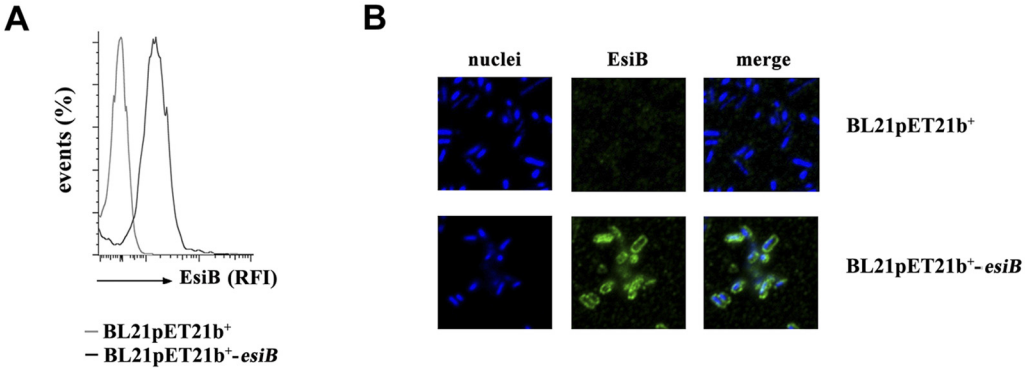

FIG 4 Constitutive expression of EsiB in strain BL21::*esiB* postulates the exposure of the protein on the bacterial surface. (A) EsiB expression in the BL21::*esiB* strain was evaluated by flow cytometry, using the *E. coli* BL21(DE3) strain as a negative control. The histogram represents a typical experiment out of two performed with similar results. RFI, relative fluorescence intensity. (B) Confocal microscopy of EsiB surface localization in BL21 wild-type (top) and BL21::*esiB* (bottom) strains. Fixed bacteria were incubated with an anti-EsiB serum and then with the fluorescent secondary antibodies.

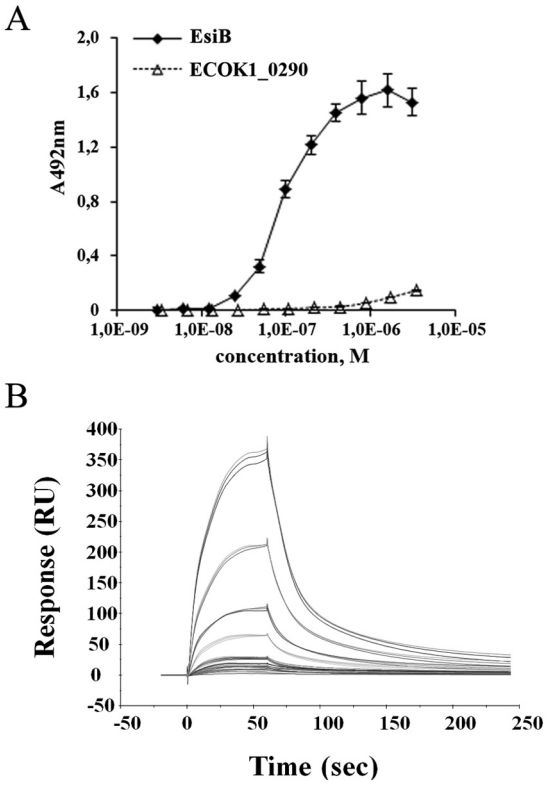

FIG 5 EsiB is able to bind to human SIgA. (A) ELISA plates were coated with SIgA and incubated with a dilution series of EsiB. Binding of EsiB was detected using mouse anti-EsiB monoclonal antibodies and peroxidase-conjugated rabbit anti-mouse IgG. ELISA data show that EsiB is able to bind human SIgA with an estimated dissociation constant of approximately 10^{-7} M. SIgA binding to an unrelated *E. coli* antigen (ECOK1_0290) was used as a negative control. The graph represents a typical experiment out of three performed with similar results. (B) Solution-phase EsiB-SIgA binding measured by surface plasmon resonance (BIAcore). Representative BIAcore sensorgrams show the response over time (resonance units [RU]) during the binding of purified recombinant EsiB to immobilized SIgA antibodies. An overlay of three repeated titration series is shown. Fitting by a 1:1 Langmuir model of the collected sensorgrams gave the following averaged kinetic constants: k_{on}, 1.39×10^3 M^{-1} s^{-1}; k_{off}, 4.2×10^{-2} 1/s; K_d, 3.02×10^{-5} M.

binding to SIgA, we investigated the antigen capability to interfere with antibody effector functions.

As SIgA can induce superoxide generation by PMNs *in vitro* (3), we first assessed the ability of EsiB to hamper the SIgA-mediated triggering of a respiratory burst in neutrophils, characterized by NADPH oxidase activation and degranulation, which can be measured in a chemiluminescence assay (12). Interestingly, we observed that EsiB is capable of blocking the SIgA-triggered oxidative burst at concentrations greater than 1 μg/ml, in a dose-dependent manner (Fig. 7A). In particular, a concentration of 20 μg/ml was sufficient to cause approximately 80% inhibition of ROS production after 30 min of incubation at 37°C (Fig. 7B). Moreover, EsiB did not inhibit a phorbol 12-myristate 13-acetate (PMA)-induced respiratory burst (data not shown), suggesting that its inhibitory effect is specific for SIgA stimulation. Together, these data indicate that EsiB can block the SIgA-triggered oxidative burst, which may be advantageous to the pathogen.

Considering that cross-linking of FcαRI on neutrophils also leads to the release of different chemotactic factors (13), to further assess the physiological relevance of EsiB interaction with SIgA, we tested its ability to interfere with neutrophil migration. Using supernatants deriving from PMN incubation with SIgA or EsiB-treated SIgA as a source of chemotactic stimuli, we quantified neutrophil migration by flow cytometry and found that EsiB, used at a concentration of 30 μg/ml, is able to cause approximately 40% inhibition of chemotaxis (Fig. 7C). These data suggest that EsiB can induce a decreased recruitment of neutrophils at the infection site, which results in avoiding clearance.

EsiB impairs FcαRI-mediated neutrophil activation. IgA-BPs usually allow bacteria to evade IgA-driven eradication processes by blocking the interaction of IgA with FcαRI. Therefore, to elucidate the mechanism of action of EsiB, we investigated the antigen capacity to block this interaction. SIgA was preincubated with EsiB before addition to neutrophils, and cells were then stained with a fluorescein isothiocyanate (FITC)-labeled anti-human IgA antibody. Flow cytometric analysis revealed that EsiB is able to bind SIgA and that this interaction does not prevent SIgA binding to neutrophils (data not shown), suggesting that EsiB most likely binds to a region on SIgA not overlapping with the FcαRI binding site. EsiB used as a negative control did not bind to cells (data not shown), showing that the inhibition of SIgA-mediated eradication processes was not due to a direct effect of the protein on neutrophils. Together, these data indicate that, unlike most bacterial IgA-BPs, EsiB does not inhibit SIgA-FcαRI complex formation.

Since SIgA binding to PMNs was not hampered by EsiB, we hypothesized that the inhibition of antibody effector functions could be due to EsiB preventing productive FcαRI cross-linking, which is crucial for initiation of signal transduction pathways that lead to neutrophil activation.

To understand whether EsiB could interfere with FcαRI signaling, we analyzed the general tyrosine phosphoprotein pattern in neutrophils stimulated with SIgA alone or in combination with EsiB, and we observed that preincubation with EsiB results in a dose-dependent decrease in the phosphorylation level of different cytoplasmic proteins (Fig. 8A), including phospholipase C-γ (PLC-γ), which has been reported to participate in signal transduction pathways involved in activation of NADPH oxidase and chemotaxis (14). Neutrophil stimulation with EsiB alone did not result in cell activation (data not shown), consistent with the inability of the antigen to bind to PMNs.

To further investigate whether EsiB could selectively affect downstream components of FcαRI signaling, we focused on two members of the mitogen-activated protein kinase (MAPK) family specifically implicated in neutrophil responses: the extracellular signal-regulated kinases 1 and 2 (ERK1/2), involved in cell survival and proliferation, and the stress-activated kinase p38, participating in respiratory burst activity and chemotaxis (15). The analysis of MAPK activation using phosphospecific antibodies showed that EsiB is able to impair, in a dose-dependent manner, FcαRI-dependent phosphorylation of ERK1/2 and p38 (Fig. 8B to D). Collectively, these data suggest that EsiB can interfere with a productive FcαRI signaling, resulting in the inhibition of SIgA effector functions.

DISCUSSION

In this study, we functionally characterized EsiB, an *E. coli* antigen (previously annotated as c5321) proposed as a candidate for an

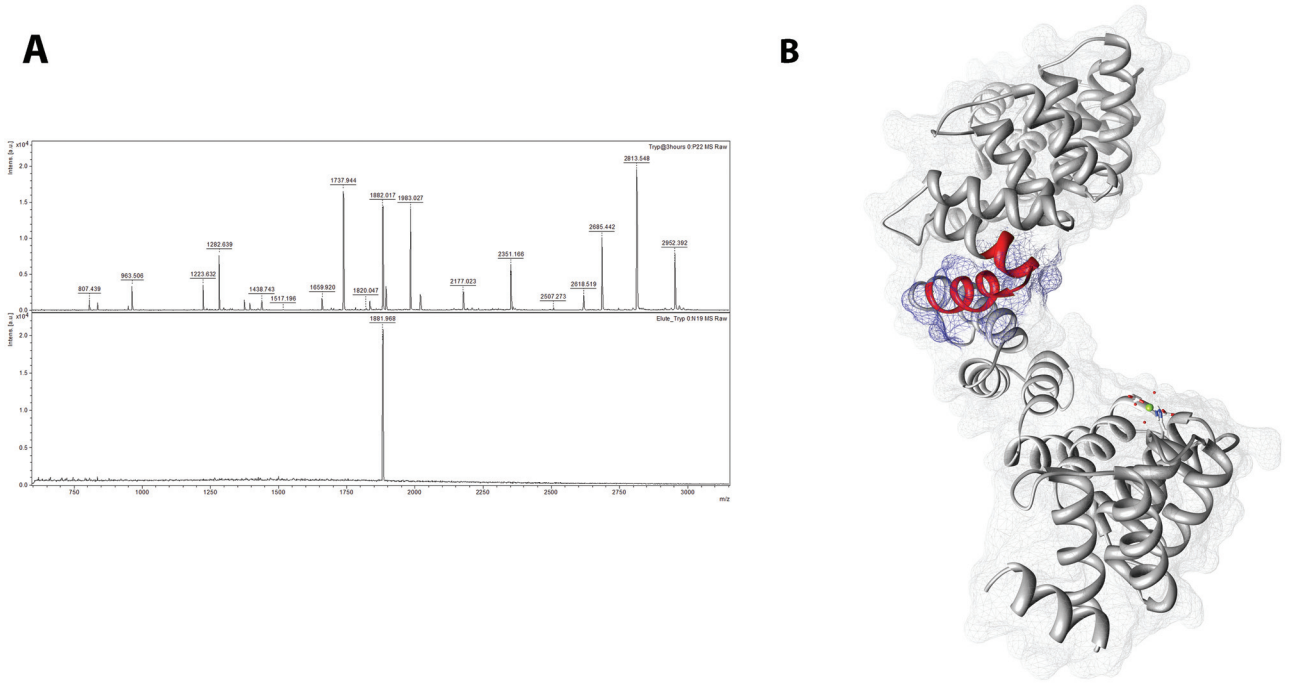

FIG 6 Identification of the EsiB IgA-binding motif. (A) Mass spectra obtained during the immunocapturing procedure. The upper spectrum shows the peptide mixture obtained after EsiB digestion with trypsin, and the lower spectrum shows the captured peptide with an *m/z* of 1,881.968. This peptide corresponds to the segment 244-VLFSQSAEQGNSIAQFR-260. (B) The position of the identified peptide is shown in red on the EsiB structure (PDB entry 4BWR) (Urosev et al., submitted).

ExPEC vaccine (5). The recent availability of structural data (Urosev et al., submitted) has raised new perspectives on the possible involvement of EsiB in *E. coli* pathogenesis and evasion of host immune responses. This hypothesis was in part supported by the analysis of human sera, which showed that patients suffering from UTIs possessed IgG titers against the antigen significantly higher than titers in healthy individuals, suggesting that EsiB triggers an *in vivo* immune response during *E. coli* infection of the urinary tract. This is in agreement with the fact that the *esiB* gene was prevalently associated with ExPEC strains (B2 group), with uropathogenic pathotypes being the most well represented. The fact that EsiB was expressed by bacteria in a detectable amount only under *in vivo* infection conditions suggests that the antigen may have a role during a specific stage of pathogenesis, although the regulatory mechanism remains unknown. The antibacterial defense of the urinary tract depends on two key players: neutrophils, which are crucial effectors of innate immunity, and SIgA, which not only prevents pathogen adherence to mucosal surfaces but also triggers a wide variety of elimination mechanisms elicited upon cross-linking of FcαRI on neutrophils, including the activa-

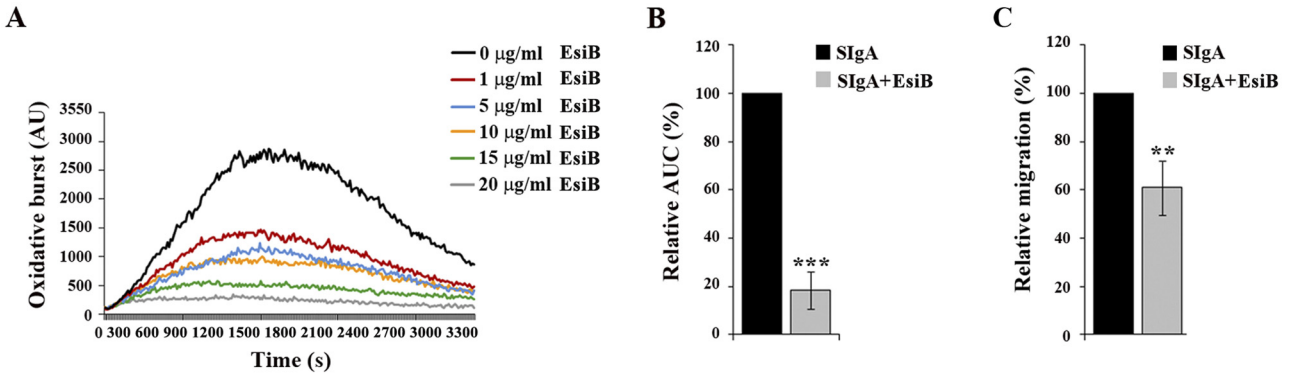

FIG 7 EsiB inhibits SIgA effector functions. (A) EsiB inhibits the SIgA-mediated neutrophil oxidative burst in a dose-dependent manner. ROS production by PMNs was measured by chemiluminescence every 30 s for 60 min at 37°C and quantified in arbitrary units (AU). The graph represents a typical experiment out of five performed with similar results. (B) ROS production at 30 min is shown as relative area under the curve (AUC), in the presence of 20 μg/ml of EsiB. (C) EsiB inhibits the SIgA-induced neutrophil chemotaxis. To measure neutrophil chemotaxis, bottom chambers of Transwell supports were filled with supernatants deriving from PMNs incubated with SIgA or EsiB-treated SIgA. Neutrophils were added to the upper chambers. After 1 h at 37°C, cells that had migrated toward the lower compartments were quantified by flow cytometry. The graph represents a typical experiment out of three performed with similar results. ***, $P \leq 0.001$; **, $P \leq 0.01$. Error bars, SD.

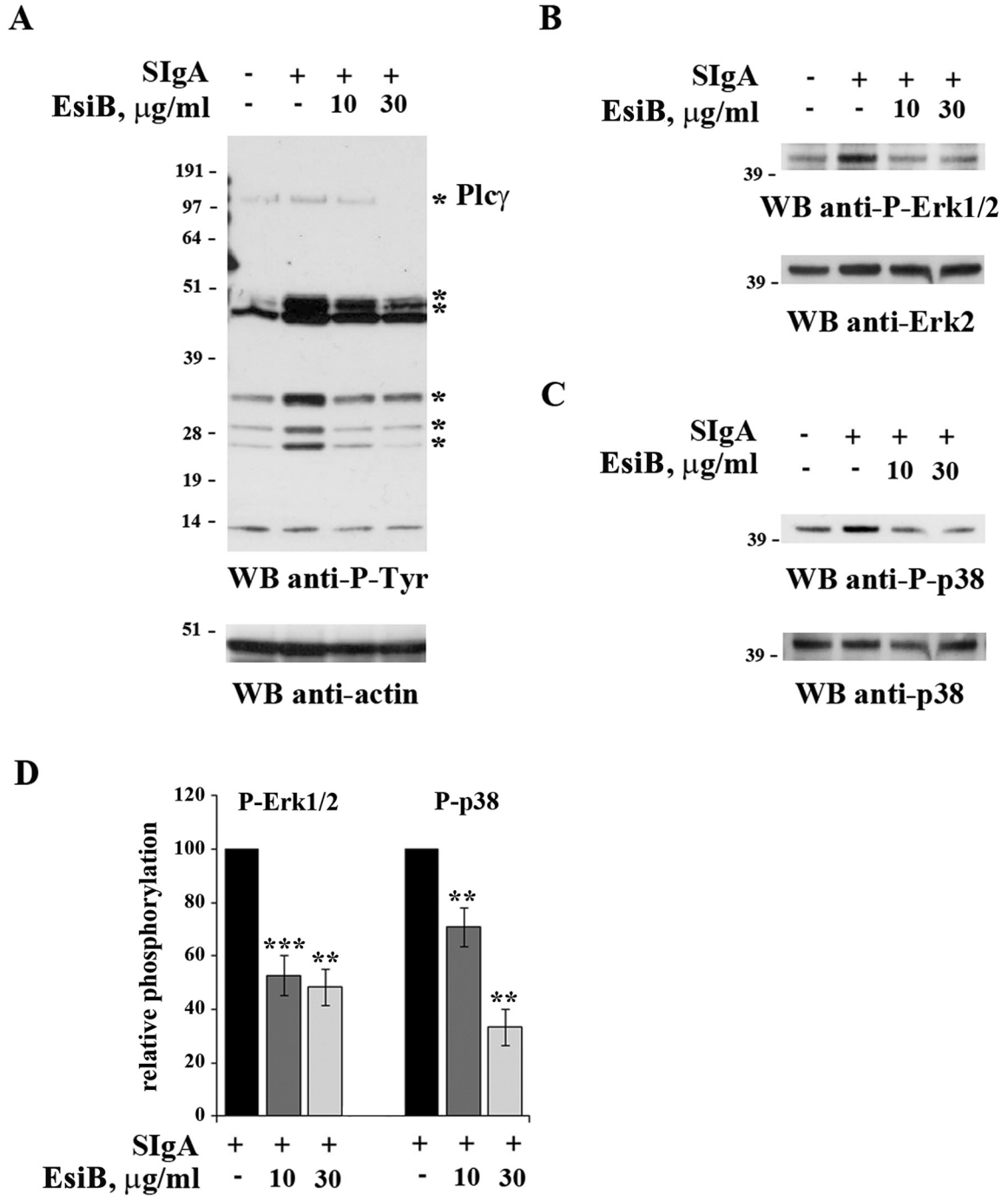

FIG 8 EsiB interferes with FcαRI signaling. (A) Neutrophil activation was performed by incubating cells with SIgA or EsiB-treated SIgA for 1 min at 37°C. Cells were lysed in 1% Triton X-100 in 20 mM Tris-HCl, pH 8.0, 150 mM NaCl, in the presence of a protease inhibitor cocktail. Equal amounts of proteins from each sample were resolved by 10% SDS-PAGE and transferred to 0.45-μm nitrocellulose filters. Immunoblot assays were carried out using antiphosphotyrosine antibody and peroxidase-conjugated rabbit anti-mouse antibody. Blots were reprobed with loading control antibody after stripping (antiactin). The positions of molecular mass markers (kDa) are indicated on the left. The interaction of EsiB with SIgA resulted in dose-dependent modifications in the tyrosine phosphorylation level of specific cytosolic proteins, including PLC-γ and others not yet identified (*). PLC-γ identity was confirmed by reprobing the blot with anti-PLC-γ1 antibody after stripping (data not shown). The blot represents a typical experiment out of three performed with similar results. (B and C) Immunoblot analysis, using a phosphospecific antibody, of ERK1/2 (B) and p38 (C) phosphorylation in neutrophils stimulated with SIgA or EsiB-treated SIgA. Filters were stripped and reprobed with control anti-ERK (B) and anti-p38 (C) antibodies. The results of a representative experiment are shown. (D) Quantification by laser densitometry of the relative levels of ERK1/2 phosphorylation (the ERK1/2 phosphorylation in control cells was defined as 100%) and p38 phosphorylation (the p38 phosphorylation in control cells was defined as 100%). EsiB affected to a significant extent the basal level of both ERK1/2 and p38 phosphorylation. ***, $P \leq 0.001$; **, $P \leq 0.01$. Error bars, SD.

tion of a respiratory burst and the release of cytokines, chemotactic factors, and inflammatory lipid mediators (9, 11). The evidence that numerous pathogens have evolved mechanisms to specifically evade or subvert the IgA immune response is an indicator of the importance of IgA in protection against infection. These evasion mechanisms include proteins that bind specifically to IgA, inhibiting its action, as well as specific proteases that inactivate IgA through cleavage (10). Important examples of IgA-BPs include proteins Arp4 and Sir22 of group A *Streptococcus*, which are members of the M protein family (16, 17), and β-protein, an unrelated protein expressed by group B *Streptococcus* (18, 19). These streptococcal proteins interact with the IgA Cα2-Cα3 domain interface, which is essentially the same site recognized by FcαRI. Therefore, the IgA-BPs can inhibit IgA binding to FcαRI, as well as the triggering of the FcαRI-mediated respiratory burst (12). Another example of IgA-BP is represented by staphylococcal superantigen-like 7 (SSL7), a secreted toxin of *Staphylococcus aureus* which is able to bind monomeric IgA1 and IgA2 and also SIgA, competitively inhibiting FcαRI binding (20). Our finding that SIgA, the predominant antibody in the urinary tract secretions (10), is a crucial interactor with EsiB contributing to its immunomodulatory properties is of particular relevance to *E. coli* pathogenesis. Although we demonstrated that the cognate interaction of EsiB with SIgA is associated with a single peptide containing the E251 amino acid, we were not able to map the SIgA region bound by the antigen. Indeed, MS/MS analysis of a tryptic digest of purified SIgA immobilized on a chip and then incubated with EsiB revealed no interaction with isolated Fab or Fc portions, suggesting that a complete immunoglobulin is required for the binding (data not shown). Although the affinity constant of EsiB for SIgA is relatively low (K_d of approximately 10^{-7} M), it is conceivable that the avidity effect caused by the interaction of EsiB with multiple binding sites on SIgA may increase the local affinity, which was evaluated here as a 1:1 interaction. It can be difficult to predict whether during specific physiological events, affinity constants measured *in vitro* would correlate with the capacity of an antigen to sequester target molecules. However, we suggest that the interaction of EsiB with SIgA should at least imply high local concentrations of EsiB or the modulation of SIgA binding by other factors.

EsiB, unlike most bacterial IgA-BPs, cannot block cell surface binding of SIgA to FcαRI, which is in agreement with the antigen incapability of binding to the isolated Fc region of SIgA. However, we showed that EsiB was able to inhibit the antibody effector functions, such as superoxide generation and cellular migration, by interfering with the SIgA-triggered neutrophil activation. Indeed, EsiB interaction with SIgA was able to significantly decrease the tyrosine phosphorylation level of neutrophil PLC-γ, ERK1/2, and p38, which are all downstream components of the FcαRI signal transduction pathway that leads to cell activation. These data strongly suggest that EsiB can prevent productive FcαRI cross-linking by SIgA on the neutrophil plasma membrane, thus inhibiting the recruitment of immune cells at the infection site and the ROS-mediated killing of the pathogen.

To our knowledge, this study represents the first report of an *E. coli* SIgA-binding antigen that allows the bacterium to subvert host immune responses and avoid clearance by inhibiting neutrophil activation.

MATERIALS AND METHODS

Ethics statement. The institutional review board of the Department of Health Service at Novartis Vaccines and Diagnostics (Siena, Italy) approved the study and the use of human samples from the volunteers. Written, informed consent was obtained from the adult participants.

Cells, antibodies, and reagents. Polymorphonuclear neutrophils (PMNs) were purified from buffy coats from anonymous healthy donors (available from authorized blood banks) by density gradient centrifugation (400 $\times$ *g* for 30 min at room temperature) on Ficoll-Paque Plus (GE Healthcare), followed by centrifugation (250 $\times$ *g* for 10 min at 4°C) on a 3% (wt/vol) dextran solution (Sigma-Aldrich). After osmotic lysis of erythrocytes, cells were resuspended in RPMI 1640 (Invitrogen) supplemented with 10% fetal bovine serum (FBS) (Invitrogen) and incubated at 37°C in a humidified atmosphere with 5% CO_2.

Anti-EsiB polyclonal antibodies were raised in rabbits upon immunization with the purified recombinant protein. The anti-EsiB monoclonal antibody (MAb) was made from a hybridoma produced from a mouse immunized with highly purified EsiB. The antibody, which recognizes a linear epitope in the protein, was protein G purified from the hybridoma supernatant. Antiphosphotyrosine and antiactin MAbs were purchased from Millipore. Phosphospecific antibodies recognizing the phosphorylated active forms of ERK1/2 (T202/Y204) and p38 (T180/Y182) were from Cell Signaling Technology. Polyclonal anti-ERK2 and anti-p38 antibodies were obtained from Santa Cruz Biotechnology. Alkaline phosphatase-, peroxidase-, and FITC-labeled secondary antibodies were purchased from Dako. Alexa Fluor 488-labeled secondary antibody was from Invitrogen. FITC-labeled anti-human IgA antibody was obtained from Sigma-Aldrich.

Bacterial strains and culture conditions. A total of 267 *E. coli* strains, including ExPEC (n = 119), InPEC (n = 117), and nonpathogenic (n = 31) strains, were analyzed (see Table S1 in the supplemental material). Genomic DNA was isolated using the GenElute bacterial genomic DNA kit (Sigma) according to the manufacturer's instructions and kept at 4°C until further use. Uropathogenic *E. coli* (UPEC) strain CFT073 (serotype O6:K2:H1), isolated from the blood and urine of a patient with acute pyelonephritis (21), and isogenic mutant strain CFT073Δ*esiB* were used for real-time quantitative reverse transcription-PCR (RT-PCR) studies. Strains were cultured in Luria-Bertani (LB) broth (10 g/liter tryptone, 5 g/liter yeast extract, 10 g/liter NaCl) at 37°C with agitation and aeration, and approximately 10^9 bacteria were collected after 2 h (log phase) and 5 h (stationary phase) for RNA isolation. *E. coli* DH5α-T1R (Invitrogen) was used for cloning purposes, and *E. coli* BL21(DE3) (Invitrogen) was used for expression of His-tagged fusion proteins. The clones carrying a specific cassette conferring antibiotic resistance were grown in the presence of kanamycin (50 μg/ml) or ampicillin (100 μg/ml).

Distribution analysis of the *esiB* gene. To analyze the *esiB* gene prevalence, we performed a PCR screening approach, using primers EsiB_For, CGACTGGTTAGACAGGGATAAG, and EsiB_Rev, AGGAAAAGCAAA AGGCGAGG, designed in the external conserved region. For the distribution studies, the reaction mixture, containing a final volume of 25 ml and 100 μg of genomic DNA, was prepared using GoTaq Green Master Mix (Promega). The samples were subjected to 30 cycles of amplification in a thermal cycler (GeneAmp PCR system 9700; Applied Biosystems). Reaction conditions were 10 min of initial denaturation at 94°C, followed by 30 cycles of denaturation (30 s at 94°C), annealing (30 s for 55°C), and elongation (90 s at 72°C) and a final elongation at 72°C for 10 min. The expected PCR product was 1,770 bp. Additionally, BLAST analysis was performed on publicly available whole-genome sequences of *E. coli* strains (ftp://ftp.ncbi.nih.gov/genbank/genomes/Bacteria/; see Table S1 in the supplemental material) to detect the *esiB* gene.

Cloning, expression, and purification of EsiB. The *esiB* gene, both with and without the predicted signal sequence, was amplified by PCR from the CFT073 genomic DNA template, cloned in the pET-21b vector (Novagen), and transformed in DH5α-T1R chemically competent cells for propagation. BL21(DE3) chemically competent cells were used for

His-tagged protein expression. Purification of the recombinant protein, without signal peptide, was performed from the bacterial soluble fraction using nickel-affinity chromatography as already described (22, 23).

RNA purification and real-time quantitative RT-PCR. Prior to RNA isolation, 2 volumes of RNA Protect bacterial reagent (Qiagen) was added to 1 volume of bacterial culture to immediately stabilize the *in vivo* gene expression profile in bacteria. For total RNA extraction, cells were disrupted by treatment with 15 mg/ml lysozyme (Sigma-Aldrich) and 2 mg/ml proteinase K (Qiagen) for 10 min at room temperature. RNA isolation was completed with the RNeasy minikit (Qiagen) according to the manufacturer's instructions. RNA concentration and integrity were assessed by measurement of the A_{260}/A_{280} ratios and electrophoretic analysis. Prior to RT-PCR, contaminating DNA was removed from RNA samples by treatment with RQ1 RNase-free DNase (Promega). RT-PCR was carried out on 500 ng total RNA using ImProm-II reverse transcriptase (Promega) and random primers (Promega) for first-strand cDNA synthesis.

Real-time quantitative PCR was performed using FastStart Universal SYBR Green Master (Rox) (Roche Diagnostics) in a LightCycler 480 II real-time PCR system (Roche Diagnostics). All samples were run in duplicate on 96-well optical PCR plates (Roche Diagnostics). The specific primers used to amplify cDNA fragments corresponding to EsiB mRNA and 16S rRNA were 5′ AAAGATGAGCAACAGGCCGCAATC 3′ (forward) and 5′ ATCACGTTCTACGCCCAAGCCATA 3′ (reverse) for EsiB and 5′ ACGTGCTACAATGGCGCATA 3′ (forward) and 5′ TCATGGA GTCGAGTTGCAGA 3′ (reverse) for 16S rRNA. After an initial denaturation at 95°C for 10 min, denaturation in the subsequent 40 cycles was performed at 95°C for 15 s, followed by primer annealing at 60°C for 30 s and a final extension at 72°C for 30 s. The specificity of the amplified fragments was demonstrated by the melting curve, where a single peak was observed for each sample amplified with EsiB and 16S rRNA primers. After amplification, data analysis was performed using LightCycler 480 1.5 software (Roche Diagnostics). For relative quantification of gene expression, the starting mRNA copy number of the unknown samples was determined using the comparative threshold cycle ($\Delta\Delta C_T$) method, as previously described (24), and levels of the different transcripts were normalized to 16S rRNA, used as a housekeeping gene. For absolute quantification, serial dilutions of an external homologous standard (plasmid DNA carrying the cloned target sequence) were used to generate a standard curve, and data analysis was performed using the second derivative maximum method.

Measurement of serum IgG titers against EsiB. Anti-EsiB immunoglobulin G (IgG) titers of patient sera were measured by enzyme-linked immunosorbent assay (ELISA). Briefly, Nunc-Immuno MaxiSorp 96-well plates (Thermo, Fisher Scientific) were coated overnight at 4°C with 0.5 μg of recombinant protein EsiB diluted in phosphate-buffered saline (PBS). After blocking with a 3% (wt/vol) polyvinylpyrrolidone (PVP) solution for 1 h at 37°C, plates were incubated with diluted patient sera for 2 h at 37°C. Bound IgG molecules were detected using alkaline phosphatase-conjugated goat anti-human IgG antibodies (Sigma-Aldrich), followed by the addition of a chromogen-substrate solution containing *p*-nitrophenylphosphate (Sigma-Aldrich). After 30 min, the reaction was stopped with 4 N NaOH and the absorbance at 405 nm was measured.

Binding of EsiB to SIgA (ELISA). EsiB binding to human secretory immunoglobulin A (SIgA) was measured by ELISA. Briefly, Nunc-Immuno MaxiSorp 96-well plates (Thermo, Fisher Scientific) were coated overnight at 4°C with 1 μg of human colostrum IgA (Sigma-Aldrich) diluted in PBS. After blocking with a 3% (wt/vol) PVP solution for 2 h at 37°C, plates were incubated with serially diluted recombinant EsiB for 2 h at 37°C. Bound EsiB was detected using mouse anti-EsiB monoclonal antibodies and peroxidase-conjugated rabbit anti-mouse IgG antibodies (Dako), followed by the addition of a chromogen substrate solution containing *o*-phenylenediamine dihydrochloride (Sigma-Aldrich). After 20 min, the reaction was stopped with a 12.5% (vol/vol) H_2SO_4 solution and the difference between absorbance at 492 nm and absorbance at 630 nm was measured.

Binding of EsiB to SIgA (SPR). The interaction between EsiB and secretory IgA antibodies was studied by surface plasmon resonance (SPR) using a BIAcore T200 instrument (GE Healthcare). Commercial secretory IgA antibodies (Sigma) were covalently immobilized by amine coupling on a carboxymethylated dextran sensor chip (CM-5; GE Healthcare). Amine-coupling reactions for immobilization of IgAs were performed using the purified commercial antibodies that have been previously exchanged in PBS buffer. SIgAs at ~10 μg/ml in 10 mM sodium acetate buffer, pH 5, were injected at 5 μl/min until ~1,800 response units (RU) was captured. The blank (reference) surface was constructed similarly, except that antibodies were omitted.

Running buffer containing phosphate-buffered saline (PBS) with 0.05% Tween 20 (pH 7.4) was used, and EsiB protein at a concentration range of 20 to 0.15 μM was injected. Injections were performed at 25°C with flow rates of 50 μl/min. Following each 60-s injection, a long dissociation time of 600 s allowed sensor chip surfaces to return to baseline without the need of a regeneration step. At least one concentration was included as replicate during each titration. SPR data were analyzed using the BIAcore T200 evaluation software (GE Healthcare). Titration experiments were performed in triplicate, and each sensorgram was fitted with the 1:1 Langmuir binding model, including a term to account for potential mass transfer, to obtain the individual k_{on} and k_{off} kinetic constants; the individual values were then combined to derive the single averaged K_d value reported.

Epitope mapping of SIgA-binding site on EsiB. Epitope mapping experiments were carried out with recombinant EsiB and SIgA. To this aim, we adopted and extended an immunocapturing approach successfully used previously with monoclonal antibodies (25). The approach involves proteolytic digestion (using diverse proteases) of the target antigen prior to immunocapturing and subsequent analysis of antibody-bound peptides (containing the epitope) by mass spectrometry. In order to identify the region of interaction between SIgA and EsiB, we have used the Dynabeads antibody coupling kit (catalog no. 143.11D; Invitrogen). This kit allows covalent immobilization of antibodies (or other protein ligands such as functional enzymes, etc.) onto the surface of Dynabeads. Antibody-coupled Dynabeads can then be used for downstream assays and experiments like immunoassays, immune precipitation, coimmunoprecipitation of protein complexes, etc. Captured proteins or protein complexes are easily separated from the sample using the magnetic separation properties of Dynabeads. Magnetic separation facilitates washing, buffer changes, and elution. Secretory IgA was coupled onto the surface of Dynabeads, and these were then used to capture the epitope-containing peptide. Peptide mixtures of EsiB were obtained by partial digestion with trypsin and GluC, independently, in 100 mM ammonium bicarbonate buffer at 37°C for 3 h. The immunocapturing procedure was carried out as described previously (26). Briefly, a 25-μl suspension of SIgA-coated beads was washed twice with PBS using a magnet and resuspended to the initial volume. An 0.5-μl amount of protease inhibitor mixture (GE Healthcare) was added to the beads prior to the peptide mixture to avoid potential degradation of the antibodies. On addition of the peptide mixture, the sample was incubated for 30 min at room temperature with gentle tilting and rotation. After incubation, the beads were washed three times with 1 ml of PBS, and the bound peptide was then eluted with 50 μl of 0.2% trifluoroacetic acid (TFA). In order to obtain a suitable sample for mass spectrometry analysis, elute fractions were desalted and concentrated using C_{18} ZipTips (Millipore). For the identification of the captured peptides, an ultrafleXtreme (Bruker Daltonics, Bremen, Germany) matrix-assisted laser desorption ionization–tandem time of flight (MALDI-TOF/TOF) mass spectrometer was used. For MALDI analysis, 1 μl of sample was mixed with the same volume of a saturated solution of α-cyano-4-hydroxy-*trans*-cinnamic acid matrix (0.5 mg/ml in water-acetonitrile-trifluoroacetic acid, 1%, 6:3:1) and spotted onto a MALDI target plate (Bruker). The drop was air dried at room temperature.

MALDI mass spectra were recorded in the positive ion mode, and ion acceleration was set to 25 kV. All mass spectra were externally calibrated using a standard peptide mixture (Bruker); calibration was considered good when a value below 1 ppm was obtained. For peptide mass fingerprinting analysis, the Mascot search engine (Matrix Science) was used with the following parameters: two missed cleavage permission, 10-ppm measurement tolerance. Methionine oxidation was set as a variable modification. Common contaminants were removed using the contaminant database available in the Mascot search engine. Searches were carried out using the NCBInr NC_000908.2 database. For MS/MS analysis, measurement tolerance was set to 50 ppm for MS and to 0.2 Da for MS/MS. Positive identifications were accepted with a Mascot score higher than that corresponding to a *P* value of 0.05.

Binding of SIgA and EsiB to neutrophils. To measure SIgA and EsiB binding to neutrophils, 5×10^5 cells were incubated with different concentrations of SIgA or EsiB in Hanks' balanced salt solution (HBSS) in 96-well culture plates for 20 min at 37°C. Cells were then washed and incubated for 30 min on ice with FITC-labeled anti-human IgA secondary antibody for SIgA detection or with anti-EsiB MAb followed by FITC-labeled secondary antibody for EsiB detection. For competition experiments, SIgA was preincubated with EsiB for 15 min at 37°C before addition to cells. Cell staining was analyzed by flow cytometry.

Confocal microscopy analysis of *E. coli* strains adhering to tissues. Confocal imaging on tissues was performed on bladder sections derived from ExPEC-infected animals. In detail, the bladder was cut transversely, preserved in 10% formalin (pH 7.2), and embedded in paraffin. Tissue sections were cut and mounted onto slides. Samples were dewaxed and subjected to antigen retrieval before the immunofluorescence labeling. Staining of the sections was done by using a rabbit anti-EsiB serum followed by a donkey anti-rabbit IgG conjugated to rhodamine red X as a secondary antibody. Alexa Fluor dye-labeled phalloidins (Invitrogen) were used to stain the actin cytoskeleton according to the manufacturer's instructions. Bacterial and cellular DNA was stained with 4′,6-diamidino-2-phenylindole (DAPI). The ProLong Gold reagent (Invitrogen) was used as liquid mounting. The CFT073 strain was detected using the polyclonal rabbit anti-CFT073 and the Alexa Fluor 488-conjugated goat anti-rabbit IgG secondary antibody. Tissues were labeled with wheat germ agglutinin (WGA) and conjugated with Alexa Fluor 647 (Invitrogen). The analysis was done with a Zeiss LSM 710 laser scanning microscope.

Respiratory burst measurement. PMN respiratory burst activity was measured by chemiluminescence. Briefly, neutrophils were diluted to a final concentration of 10^5 cells/ml in HBSS containing 0.1% human serum albumin (HSA). SIgA and EsiB-treated SIgA were then mixed with neutrophils. Following addition of luminol-balanced salt solution (LBSS), the oxidative burst was measured every 30 s for 60 min at 37°C by chemiluminescence using a luminometer (Berthold Technologies, Wildbad, Germany).

Chemotaxis assay. To measure neutrophil chemotaxis (directed migration), bottom chambers of Transwell supports were filled with supernatants deriving from PMNs incubated for 20 min at 37°C with SIgA or EsiB-treated SIgA. Neutrophils (2.5×10^5) were added to the upper chambers. After 1 h at 37°C, cells that had migrated toward the lower compartments were quantified by flow cytometry.

Cell activation, lysis, and immunoblot assays. Neutrophil activation by FcαRI cross-linking was performed by incubating cells (5×10^6) in HBSS with SIgA or EsiB-treated SIgA for 1 min at 37°C. Cells were recovered by centrifugation (16,000 × *g* for 30 s at 4°C), washed twice in PBS, and lysed in 1% (vol/vol) Triton X-100 in 20 mM Tris-HCl, pH 8.0, 150 mM NaCl, in the presence of a protease inhibitor cocktail (0.2 mg/ml sodium orthovanadate, 1 μg/ml pepstatin, 1 μg/ml leupeptin, 1 μg/ml aprotinin, and 10 mM phenylmethylsulfonyl fluoride). Equal amounts of proteins from each sample (measured using the Bio-Rad DC protein assay kit) were resolved by 10% sodium dodecyl sulfate-polyacrylamide gel electrophoresis (SDS-PAGE) and transferred to 0.45-μm nitrocellulose filters (Bio-Rad). Prestained molecular mass markers (Invitrogen) were included in each gel. Immunoblotting was performed using primary antibodies and peroxidase-labeled secondary antibodies according to the manufacturer's instructions and using a chemiluminescence detection kit (Thermo, Fisher Scientific). All blots were reprobed with loading control antibodies after stripping.

Statistical analysis. Mean values, standard deviations, and the *P* values associated with two-tailed unpaired Student's *t* test were calculated using the Microsoft Excel application. A level of $P < 0.05$ was considered statistically significant.

Protein structure accession number. The crystal structure of EsiB was deposited in the PDB under accession no. 4BWR.

SUPPLEMENTAL MATERIAL

Supplemental material for this article may be found at http://mbio.asm.org/lookup/suppl/doi:10.1128/mBio.00206-13/-/DCSupplemental.

Figure S1, DOCX file, 0.3 MB.
Figure S2, DOCX file, 0.1 MB.
Figure S3, DOCX file, 0.1 MB.
Table S1, PDF file, 0.1 MB.

ACKNOWLEDGMENTS

This work was mainly supported by internal funding from Novartis Vaccines and Diagnostics. However, it was also partly supported by funding under both the Sixth Research Framework Programme of the European Union (reference LSHB-CT-2006-037325, BacAbs) and the EMIDA ERA-NET "Coordination of European Research on Emerging and Major Infectious Diseases of Livestock" (financed by the European Commission's Seventh Framework Programme, project no. 219235) as part of the project "Combatting colibacillosis—a genomics-based approach."

We are indebted with gratitude to Marina Cerquetti (Istituto Superiore di Sanità, Rome, Italy) for kindly providing ExPEC clinical isolates and to Lothar H. Wieler (Freie Universität, Berlin, Germany), Ulrich Dobrindt (Universität Würzburg, Germany), Ann-Mari Svennerholm (Göteborg University, Sweden), and Gad Frankel (Imperial College London, London, United Kingdom) for providing other *E. coli* isolates. We also thank Kate Seib, Scilla Buccato, and Matthew Bottomley for critical discussion of the manuscript.

REFERENCES

1. **Kaper JB, Nataro JP, Mobley HL.** 2004. Pathogenic *Escherichia coli*. Nat. Rev. Microbiol. **2:**123–140.
2. **Croxen MA, Finlay BB.** 2010. Molecular mechanisms of *Escherichia coli* pathogenicity. Nat. Rev. Microbiol. **8:**26–38.
3. **van Egmond M, Damen CA, van Spriel AB, Vidarsson G, van Garderen E, van de Winkel JG.** 2001. IgA and the IgA Fc receptor. Trends Immunol. **22:**205–211.
4. **Monteiro RC, Van De Winkel JG.** 2003. IgA Fc receptors. Annu. Rev. Immunol. **21:**177–204.
5. **Moriel DG, Bertoldi I, Spagnuolo A, Marchi S, Rosini R, Nesta B, Pastorello I, Corea VA, Torricelli G, Cartocci E, Savino S, Scarselli M, Dobrindt U, Hacker J, Tettelin H, Tallon LJ, Sullivan S, Wieler LH, Ewers C, Pickard D, Dougan G, Fontana MR, Rappuoli R, Pizza M, Serino L.** 2010. Identification of protective and broadly conserved vaccine antigens from the genome of extraintestinal pathogenic *Escherichia coli*. Proc. Natl. Acad. Sci. U. S. A. **107:**9072–9077.
6. **Dobrindt U, Blum-Oehler G, Nagy G, Schneider G, Johann A, Gottschalk G, Hacker J.** 2002. Genetic structure and distribution of four pathogenicity islands (PAI I(536) to PAI IV(536)) of uropathogenic *Escherichia coli* strain 536. Infect. Immun. **70:**6365–6372.
7. **Lloyd AL, Rasko DA, Mobley HL.** 2007. Defining genomic islands and uropathogen-specific genes in uropathogenic *Escherichia coli*. J. Bacteriol. **189:**3532–3546.
8. **Mittl PR, Schneider-Brachert W.** 2007. Sel1-like repeat proteins in signal transduction. Cell. Signal. **19:**20–31.
9. **Uehling DT, Johnson DB, Hopkins WJ.** 1999. The urinary tract response to entry of pathogens. World J. Urol. **17:**351–358.
10. **Woof JM, Russell MW.** 2011. Structure and function relationships in IgA. Mucosal Immunol. **4:**590–597.

11. **Woof JM, Kerr MA.** 2006. The function of immunoglobulin A in immunity. J. Pathol. **208:**270–282.
12. **Pleass RJ, Areschoug T, Lindahl G, Woof JM.** 2001. Streptococcal IgA-binding proteins bind in the Calpha 2-Calpha 3 interdomain region and inhibit binding of IgA to human CD89. J. Biol. Chem. **276:**8197–8204.
13. **Bakema JE, van Egmond M.** 2011. The human immunoglobulin A Fc receptor FcalphaRI: a multifaceted regulator of mucosal immunity. Mucosal Immunol. **4:**612–624.
14. **Graham DB, Robertson CM, Bautista J, Mascarenhas F, Diacovo MJ, Montgrain V, Lam SK, Cremasco V, Dunne WM, Faccio R, Cooper-smith CM, Swat W.** 2007. Neutrophil-mediated oxidative burst and host defense are controlled by a vav-PLC gamma 2 signaling axis in mice. J. Clin. Invest. **117:**3445–3452.
15. **Roux PP, Blenis J.** 2004. ERK and p38 MAPK-activated protein kinases: a family of protein kinases with diverse biological functions. Microbiol. Mol. Biol. Rev. **68:**320–344.
16. **Frithz E, Hedén LO, Lindahl G.** 1989. Extensive sequence homology between IgA receptor and M proteins in Streptococcus pyogenes. Mol. Microbiol. **3:**1111–1119.
17. **Stenberg L, O'Toole PW, Mestecky J, Lindahl G.** 1994. Molecular characterization of protein Sir, a streptococcal cell surface protein that binds both immunoglobulin A and immunoglobulin G. J. Biol. Chem. **269:**13458–13464.
18. **Hedén LO, Frithz E, Lindahl G.** 1991. Molecular characterization of an IgA receptor from group B streptococci: sequence of the gene, identification of a proline-rich region with unique structure and isolation of N-terminal fragments with IgA-binding capacity. Eur. J. Immunol. **21:** 1481–1490.
19. **Jerlström PG, Chhatwal GS, Timmis KN.** 1991. The IgA-binding beta antigen of the c protein complex of group B streptococci: sequence determination of its gene and detection of two binding regions. Mol. Microbiol. **5:**843–849.
20. **Langley R, Wines B, Willoughby N, Basu I, Proft T, Fraser JD.** 2005. The staphylococcal superantigen-like protein 7 binds IgA and complement C5 and inhibits IgA-Fc alpha RI binding and serum killing of bacteria. J. Immunol. **174:**2926–2933.
21. **Mobley HL, Green DM, Trifillis AL, Johnson DE, Chippendale GR, Lockatell CV, Jones BD, Warren JW.** 1990. Pyelonephritogenic *Escherichia-coli* and killing of cultured human renal proximal tubular epithelial-cells—role of hemolysin in some strains. Infect. Immun. **58:** 1281–1289.
22. **O'Hara AM, Shanahan F.** 2006. The gut flora as a forgotten organ. EMBO Rep. **7:**688–693.
23. **Pizza M, Scarlato V, Masignani V, Giuliani MM, Aricò B, Comanducci M, Jennings GT, Baldi L, Bartolini E, Capecchi B, Galeotti CL, Luzzi E, Manetti R, Marchetti E, Mora M, Nuti S, Ratti G, Santini L, Savino S, Scarselli M, Storni E, Zuo P, Broeker M, Hundt E, Knapp B, Blair E, Mason T, Tettelin H, Hood DW, Jeffries AC, Saunders NJ, Granoff DM, Venter JC, Moxon ER, Grandi G, Rappuoli R.** 2000. Identification of vaccine candidates against serogroup B meningococcus by whole-genome sequencing. Science **287:**1816–1820.
24. **Livak KJ, Schmittgen TD.** 2001. Analysis of relative gene expression data using real-time quantitative PCR and the 2(T)(-delta delta C) method. Methods **25:**402–408.
25. **Koehler C, Carlier L, Veggi D, Balducci E, Di Marcello F, Ferrer-Navarro M, Pizza M, Daura X, Soriani M, Boelens R, Bonvin AM.** 2011. Structural and biochemical characterization of NarE, an iron-containing ADP-ribosyltransferase from Neisseria meningitidis. J. Biol. Chem. **286:** 14842–14851.
26. **Soriani M, Petit P, Grifantini R, Petracca R, Gancitano G, Frigimelica E, Nardelli F, Garcia C, Spinelli S, Scarabelli G, Fiorucci S, Affentranger R, Ferrer-Navarro M, Zacharias M, Colombo G, Vuillard L, Daura X, Grandi G.** 2010. Exploiting antigenic diversity for vaccine design: the chlamydia ArtJ paradigm. J. Biol. Chem. **285:**30126–30138.